# Superconducting current in a ballistic double superconducting–normal-metal–superconducting structure

Magnus Hurd* and Göran Wendin†
*Department of Applied Physics, Chalmers University of Technology and University of Göteborg, S-412 96 Göteborg, Sweden*
(Received 9 August 1994)

Using the Bogoliubov–de Gennes equation, we study superconducting current in a ballistic double superconducting–normal-metal–superconducting (SNSNS) structure. There are two contributions to the current: current $I_1$ due to the discrete part of the excitation spectrum and current $I_2$ due to the continuous part of the spectrum. Bound states (Andreev levels) are associated to each normal region. If the length $L$ of the middle S region is comparable to (or smaller than) the coherence length $\xi_0$, the Andreev levels in different regions interact; if $L \gg \xi_0$ the Andreev levels are noninteracting. The interaction between the Andreev levels influences $I_1$. Moreover, $I_2$ is negligible only in the limits $L \ll \xi_0$ and $L \gg \xi_0$. We present curves for the dependence of the critical current $I_c$ on $L$ and on the pair potential of the middle S region. The pair potential of the middle S region prevents reduction of $I_c$. The effects we study will not be present in a transfer Hamiltonian approach.

## I. INTRODUCTION

Transport properties of weak superconducting structures have been under intense study since the prediction[1] and observation[2] of the Josephson effect. Superconducting heterostructures with normal-metal inclusions are examples of such weak superconducting structures.

In recent years there has been renewed interest in superconducting heterostructures. One reason is the introduction of superconductivity into mesoscopic physics.[3–5] One is then motivated by the possibility to fabricate various small structures where superconducting regions are included. Another reason is the discovery of high-$T_c$ superconductors (HTSC), whose strange properties may be explained by their intrinsically layered structure. Moreover, the mechanism of electron transport through grain boundaries of HTSC is not well understood,[6] and the ongoing discussion on the symmetry of the order parameter of HTSC is partly based on weak link experiments.[7,8]

The simplest case of a superconducting heterostructure is the ballistic superconducting–normal-metal–superconducting (SNS) junction, which has been studied by a number of authors.[3–5,9,21] The opposite case is the superconducting superlattice,[10] where the alternating S and N regions are repeated periodically. Theoretical work on superlattices rely on periodic boundary conditions which are not present when considering real finite systems. The cluster case with a small number of periods is worth studying, partly because this is closer to what is fabricated in the laboratory.

Therefore, in this paper we study a ballistic SNSNS junction. In our treatment there are no normal scattering mechanisms present. In this situation Andreev reflection makes current transport possible. It is well known that superconducting bound states with energies below the gap $\Delta$ (Andreev states) contribute to the current through SNS structures.[9] The Andreev states are localized to the normal region. Now, if there is more than one normal region, Andreev states are found in each normal region. In the SNSNS case this results in interaction between Andreev states associated with different regions. This interaction is strong if the length $L$ of the middle S region is short compared to the coherence length $\xi_0$ ($\xi_0 = k_F^{-1}\mu/\Delta$, where $k_F$ is the Fermi wave vector and $\mu$ is the Fermi energy) and small if $L \gg \xi_0$. In the superlattice case the interaction leads to broadening into a band structure of the Andreev states.[11,12] The same effects were also investigated for the bound quasiparticle states of vortices in type-II superconductivity for a dense Abrikosov lattice.[13]

We calculate the stationary supercurrent for the SNSNS structure as a function of the superconducting phase difference $\phi$, modeling the pair potential as a stepwise constant function. This means we do not use a self-consistently determined pair potential (a self-consistently determined pair potential has been used in the SNS case[14]). The lack of a self-consistent pair potential leads to violation of current conservation, a matter thoroughly discussed in Refs. 15 and 16. In the case of a point-contact geometry with a small number of modes compared to the number of modes in the wide leads, the corrections due to self-consistency are small.[16] Moreover, we concentrate on the single-mode case. This corresponds to a double point-contact geometry. However, our approach can be generalized to the multimode case.

The problem of supercurrent through a Coulomb dot (the phenomenon of Coulomb blockade) is related to the SNSNS structure we study,[17] but there are important differences. We do not include any electrostatic interaction in the middle S region. In addition we study the ballistic case, contrary to the tunneling case of Ref. 17, where the transfer Hamiltonian was used. Any detailed comparison between our work and Ref. 17 is therefore difficult to make.

In addition to the current from the bound states, there is also a current contribution from the continuous part of the excitation spectrum. We calculate this contribution using the Landauer formalism describing current transport in terms of transmission probabilities.[4,5]

 

## II. THE SNSNS JUNCTION

To determine the current of the SNSNS junction we solve the one-dimensional time-independent Bogoliubov–de Gennes (BdG) equation:[18]

$$\begin{pmatrix} \mathcal{H}_0 & \Delta(x) \\ \Delta^*(x) & -\mathcal{H}_0 \end{pmatrix} \Psi = E\Psi, \tag{1}$$

where $\Psi(x)$ is a two-component wave function and $\mathcal{H}_0 = p_x^2/2m - \mu$ is the one-electron Hamiltonian. The positive eigenvalues $E$ of Eq. (1), measured relative to the Fermi energy $\mu$, determine the excitation spectrum of the system. The cross section area of the junction is assumed to be less than the penetration depth, so that the vector potential can be neglected.[19]

The pair potential of the SNSNS system, shown in Fig. 1, is assumed to have the form

$$\Delta(x) = \begin{cases} \Delta_1 e^{-i\phi/2} & \text{if } x < 0, \\ 0 & \text{if } 0 < x < L_N, \\ \Delta_3 & \text{if } L_N < x < L_N + L, \\ 0 & \text{if } L_N + L < x < 2L_N + L, \\ \Delta_1 e^{i\phi/2} & \text{if } 2L_N + L < x. \end{cases} \tag{2}$$

We assume that the junction is symmetric, but allow the pair potential $\Delta_3$ of the middle S region to differ from the electrodes. However, throughout the paper $\Delta_3 \leq \Delta_1$. Considerations of the case $\Delta_3 > \Delta_1$ have been carried out for the asymmetric SNS system.[20] Due to current conservation, we have $\phi_5 - \phi_3 = \phi_3 - \phi_1 = \phi/2$. We are free to choose the absolute phase of the middle S region to zero.

## III. THE DISCRETE SPECTRUM

The discrete part of the excitation spectrum, meaning solutions of Eq. (1) with $E < \Delta_1$, depends on $\phi$. From this dependence we calculate the current contribution $I_1$ from the discrete spectrum:[3,5]

$$I_1 = -\frac{2e}{\hbar} \sum_n \tanh\left(E_n/2k_BT\right) \frac{dE_n}{d\phi}. \tag{3}$$

The sum in Eq. (3) is over the discrete energy levels determined from Eq. (1).

To produce wave functions of the SNSNS structure, we proceed as in Ref. 21 treating the SNS junction.

In the normal regions $j$ ($j = 2, 4$) the unnormalized eigenfunctions of Eq. (1) are

$$\Psi_{j,e}^{\pm} = \begin{pmatrix} 1 \\ 0 \end{pmatrix} \exp(\pm i q_{j,e} x), \quad q_{j,e} = k_F\sqrt{1 + E/\mu},$$
$$\Psi_{j,h}^{\pm} = \begin{pmatrix} 0 \\ 1 \end{pmatrix} \exp(\pm i q_{j,h} x), \quad q_{j,h} = k_F\sqrt{1 - E/\mu}, \tag{4}$$

where $k_F = \sqrt{2m\mu}/\hbar$. In the superconducting regions $j$ ($j = 1, 3, 5$) the unnormalized eigenfunctions of Eq. (1) are

$$\Psi_{j,e}^{\pm} = \begin{pmatrix} u_j e^{i\phi_j} \\ v_j \end{pmatrix} \exp(\pm i k_{j,e} x),$$
$$\Psi_{j,h}^{\pm} = \begin{pmatrix} v_j e^{i\phi_j} \\ u_j \end{pmatrix} \exp(\pm i k_{j,h} x), \tag{5}$$

where, if $E > \Delta_j$,

$$k_{j,e} = k_F[1 + (E^2 - \Delta_j^2)^{1/2}/\mu]^{1/2},$$
$$k_{j,h} = k_F[1 - (E^2 - \Delta_j^2)^{1/2}/\mu]^{1/2}, \tag{6}$$

or, if $E < \Delta_j$,

$$k_{j,e} = k_F[1 + i(\Delta_j^2 - E^2)^{1/2}/\mu]^{1/2}, k_{j,h} = (k_{j,e})^*, \tag{7}$$

and

$$u_j^2 = [1 + (E^2 - \Delta_j^2)^{1/2}/E]/2,$$
$$v_j^2 = [1 - (E^2 - \Delta_j^2)^{1/2}/E]/2. \tag{8}$$

Now we make the ansatz for regions 1 and 5

$$\Psi(x) = \begin{cases} c_1\Psi_{1,e}^- + d_1\Psi_{1,h}^+ & \text{if } x < 0, \\ a_5\Psi_{5,e}^+ + b_5\Psi_{5,h}^+ & \text{if } 2L_N + L < x, \end{cases} \tag{9}$$

and for the middle regions $j = 2, 3, 4$

$$\Psi(x) = a_j\Psi_{j,e}^+ + b_j\Psi_{j,h}^- + c_j\Psi_{j,e}^- + d_j\Psi_{j,h}^+. \tag{10}$$

The form of the wave functions $\Psi_1$ and $\Psi_5$ guarantees a decaying behavior when $|x| \to \infty$. We match the ansatz and the derivative of the ansatz at the interfaces. After eliminating the coefficients of the middle regions, we end up with the following equations for the coefficients $c_1$, $d_1$, $a_5$, and $b_5$:

$$M \begin{pmatrix} 0 \\ 0 \\ c_1 \\ d_1 \end{pmatrix} = \begin{pmatrix} a_5 \\ b_5 \\ 0 \\ 0 \end{pmatrix}. \tag{11}$$

$M \equiv M(E)$ is the $4 \times 4$ transfer matrix associated with the clean SNSNS structure. Besides Eq. (11) there is also a normalization condition for the wave function, which in this work is of no interest. We do not need all the components $M_{ij}$, since the condition for having nonzero solutions $c_1$, $d_1$, $a_5$, and $b_5$ is[21]

$$M_{33}M_{44} - M_{34}M_{43} = 0. \tag{12}$$

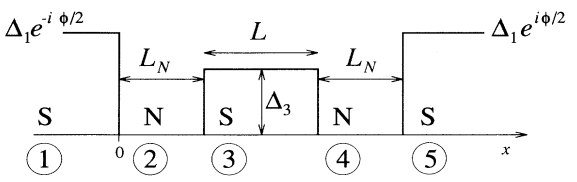


FIG. 1. Layout of the SNSNS system.

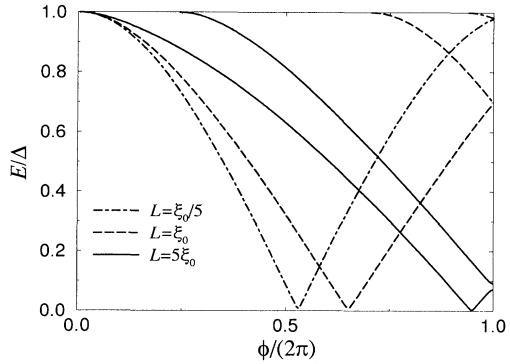


FIG. 2. Discrete levels for several lengths for the case $\Delta_1 = \Delta_3$. Note that in this figure the full $4\pi$ variation is not shown. The energy vs phase curves have even symmetry about $2\pi$.

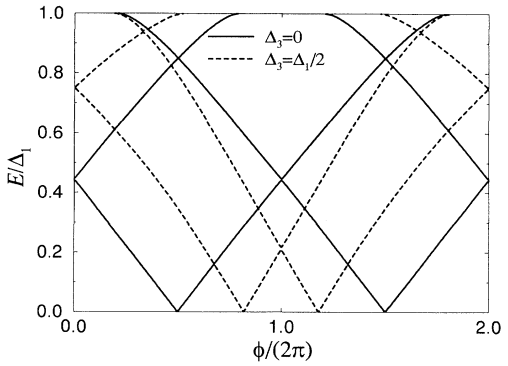


FIG. 3. Discrete levels for several values of $\Delta_3$. For both cases $L = 5\xi_0$.

Equation (12) determines the excitation spectrum for the bound Andreev levels of the SNSNS structure. We solve Eq. (12) numerically. The results are presented in Fig. 2. In all plots we have chosen $\Delta_1/\mu = 1/50$ and zero temperature.

Let us first consider the case when the pair potential in all S regions is the same, $\Delta_1 = \Delta_3 = \Delta$. In the case $L_N \gg \xi_0$, there are several Andreev levels present in the spectrum. In Fig. 2 we show the case $L_N \ll \xi_0$, when there are at most two levels present. For small length $L$ of the middle S region, we approach the short SNS junction case, as is seen in Fig. 2, with the dispersion relation $E = \Delta\,|\cos(\phi/2)|$. The small gaps in the spectrum are because of normal reflection due to a finite value of the ratio $\Delta/\mu$, as investigated in Ref. 21. We note that for $L \gg \xi_0$ the two levels approach each other and become almost degenerate with the dispersion relation $E = \Delta\,|\cos(\phi/4)|$. This is clearly due to the small overlap between the wave functions of the localized Andreev levels associated to each N region. The $\cos(\phi/4)$ dependence is easy to understand [see Eq. (2)]: when $L \gg \xi_0$ the phase difference over each junction is $\phi' = \phi/2$, giving back the usual $\cos(\phi'/2)$ dependence of a ballistic SNS junction. We would like to emphasize, however, that the general dependence of $E(\phi)$ is $4\pi$ periodic. Moreover, by analogy, a SNS $\cdots$ NS structure with $n$ periods should show $n2\pi$ periodicity of $E(\phi)$.

We also vary the pair potential $\Delta_3$ of the middle S region. The result is shown in Fig. 3. Levels disappear into the continuum when $\Delta_3$ is increasing from zero.

## IV. THE CONTINUOUS SPECTRUM

To calculate the current contribution from the continuous spectrum we use the Landauer formalism describing current transport in terms of transmission probabilities. The approach by Landauer has to be generalized to handle the superconducting case.[4,5] Since we differ from Refs. 4 and 5 we describe in detail the procedure, which is close to Ref. 22 treating NS junctions.

The first step is the introduction of the modified quasiparticle operators[1] $\gamma^\dagger_{e\mathbf{k}\sigma}$ and $\gamma^\dagger_{h\mathbf{k}\sigma}$ which change the charge by exactly $\pm e$, respectively:

$$\begin{aligned}\gamma^\dagger_{e\mathbf{k}\uparrow} &= u^*_{\mathbf{k}} c^\dagger_{\mathbf{k}\uparrow} - v^*_{\mathbf{k}} S^\dagger c_{-\mathbf{k}\downarrow} = S^\dagger \gamma^\dagger_{h\mathbf{k}\uparrow},\\ \gamma^\dagger_{e-\mathbf{k}\downarrow} &= u^*_{\mathbf{k}} c^\dagger_{-\mathbf{k}\downarrow} + v^*_{\mathbf{k}} S^\dagger c_{\mathbf{k}\uparrow} = S^\dagger \gamma^\dagger_{h-\mathbf{k}\downarrow},\end{aligned} \tag{13}$$

where $S^\dagger$ ($S$) adds (destroys) a Cooper pair to (in) the condensate. It is important to note that both types of operators exist for $k$ both greater than and less than $k_F$.[23] For $k > k_F$ the excitations have electronlike character; for $k < k_F$ the excitations have holelike character. The reason for introducing the modified quasiparticle operators in Eq. (13) is that we want to study processes where exactly $\pm e$ is transferred through the junction.

To calculate the current, one studies excitations incident on the SNSNS structure from both the left (positive group velocity) and the right (negative group velocity). In the superconducting case, it is possible to have both electronlike and holelike quasiparticles incident, as shown in Fig. 4. Let us first consider the current contribution from the electronlike branch, expressed in a Landauer-type formula:[24]

$$\begin{aligned}I^e_2 = &-e\int_{k_F}^{\infty} \frac{dk}{2\pi}\frac{\hbar k}{m}\left[T^e_{L\to R}(E_k,\phi) - T^e_{R\to L}(E_k,\phi)\right]\left[1 - f\left(E_k\right)\right]\\ &+e\int_{k_F}^{\infty} \frac{dk}{2\pi}\frac{\hbar k}{m}\left[T^e_{L\to R}(E_k,\phi) - T^e_{R\to L}(E_k,\phi)\right] f\left(E_k\right),\end{aligned} \tag{14}$$

where $T^e_{L\to R}(E_k,\phi)$ $[T^e_{R\to L}(E_k,\phi)]$ is the transmission probability for an electronlike quasiparticle incident from left (right), $E_k = \left(\epsilon_k^2 + \Delta_1^2\right)^{1/2}$ and $f\left(E_k\right) = \left[1 + \exp\left(E_k/k_BT\right)\right]^{-1}$. In Eq. (14), the first integral represents quasiparticle injections caused by $\gamma^\dagger_{h\mathbf{k}}|0\rangle$ ($|0\rangle$ is the ground state of the superconductor). The minus sign is due to the fact that $\gamma^\dagger_{h\mathbf{k}}|0\rangle$ increases the momentum of the state by $\hbar k$. The last factor of the first integral

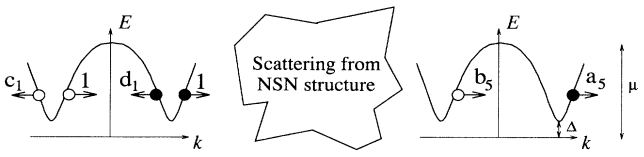


FIG. 4. Quasiparticles injected from the left. Filled (unfilled) circles correspond to electronlike (holelike) injections. In both cases the shown processes assume the Andreev approximation. Also, not shown in the figure, there are quasiparticle injections from the right.

takes into account the occupation probability for finite temperatures $T$. The second integral of Eq. (14) represents quasiparticle injections caused by $\gamma_{e\mathbf{k}}\left(\gamma^{\dagger}_{e\mathbf{k}}|0\rangle\right)$, which decrease the momentum of the state by $\hbar k$. Adding the two contributions of Eq. (14) we have

$$I_2^e = e\int_{k_F}^{\infty}\frac{dk}{2\pi}\frac{\hbar k}{m}\left[T^e_{L\to R}(E_k,\phi)-T^e_{R\to L}(E_k,\phi)\right] \times\left[2f\left(E_k\right)-1\right]. \tag{15}$$

Making use of $d\epsilon_k/dk = \hbar^2 k/m$ and $d\epsilon_k/dE_k = E_k/\left(E_k^2-\Delta_1^2\right)^{1/2}$, we rewrite Eq. (15):

$$I_2^e = \frac{e}{h}\int_{\Delta_1}^{\infty}dE\frac{E}{\sqrt{E^2-\Delta_1^2}}\left[T^e_{L\to R}(E,\phi)-T^e_{R\to L}(E,\phi)\right] \times\left[2f\left(E\right)-1\right]. \tag{16}$$

The current caused by holelike quasiparticles (see Fig. 4) incident on the structure is written, analogous to Eqs. (14) and (15),

$$I_2^h = e\int_{-k_F}^{0}\frac{dk}{2\pi}\frac{\hbar k}{m}\left(T^h_{L\to R}(E_k,\phi)-T^h_{R\to L}(E_k,\phi)\right) \times\left[2f\left(E_k\right)-1\right]. \tag{17}$$

Further simplification gives, analogous to Eq. (16),

$$I_2^h = -\frac{e}{h}\int_{\Delta_1}^{\sqrt{\mu^2+\Delta_1^2}}dE\frac{E}{\sqrt{E^2-\Delta_1^2}}\left(T^h_{L\to R}(E,\phi) -T^h_{R\to L}(E,\phi)\right)\left[2f\left(E\right)-1\right]. \tag{18}$$

Now, it remains to calculate the transmission probabilities. Investigating the continuous spectrum, we make the Andreev approximation. This approximation is valid for $\Delta_j \ll \mu$, and means that we neglect processes with large momentum changes. Within the Andreev approximation, we write down the wave function for the electronlike quasiparticle with energy $E>\Delta_1$ incident from the left, see Fig. 4. For the outer regions $j=1$ and 5 we have

$$\Psi(x)=\begin{cases}\Psi^+_{1,e}+d_1\Psi^+_{1,h} & \text{if } x<0,\\ a_5\Psi^+_{5,e} & \text{if } 2L_N+L<x,\end{cases} \tag{19}$$

and for the middle regions, $j=2,3$, and 4,

$$\Psi(x)=a_j\Psi^+_{j,e}+d_j\Psi^+_{j,h}. \tag{20}$$

Matching the wave functions at the interfaces makes it possible for us to eliminate the middle region coefficients and solve for $a_5$. To simplify, we investigate the case $L_N=0$. Then we get

$$\begin{aligned}a_5\left(E,\phi\right) &= (u^2-v^2)(u_3^2-v_3^2)/\left[u^2e^{i\phi}(u_3^2e^{-ik_{3,e}L}-v_3^2e^{-ik_{3,h}L})\right.\\ &\left.+2uvu_3v_3e^{i\phi/2}(e^{-ik_{3,h}L}-e^{-ik_{3,e}L})-v^2(u_3^2e^{-ik_{3,h}L}-v_3^2e^{-ik_{3,e}L})\right].\end{aligned} \tag{21}$$

Putting $\Delta_3=0$, we reproduce the result of Ref. 5 without an impurity.

Repeating the calculation above for a holelike quasiparticle incident on the structure (see Fig. 4), we have

$$b_5(E,\phi)=e^{i\phi}e^{-i(k_{3,e}+k_{3,h})L}a_5(E,-\phi). \tag{22}$$

The result of Eq. (22) can also be obtained by making the transformations $u_3\to v_3$, $v_3\to u_3$, $u\to v$, $v\to u$, $k_{3,e}\to -k_{3,h}$, and $k_{3,h}\to -k_{3,e}$ in Eq. (21).

Now we can write down the transmission probabilities using Eq. (22):

$$\begin{aligned}T^e_{L\to R}(E,\phi)&=\left|a_5(E,\phi)\right|^2,\\ T^h_{L\to R}(E,\phi)&=\left|b_5(E,\phi)\right|^2=\left|a_5(E,-\phi)\right|^2.\end{aligned} \tag{23}$$

In addition to Eq. (23) we have[5]

$$T^{e/h}_{R\to L}(E,\phi)=T^{e/h}_{L\to R}(E,-\phi). \tag{24}$$

Putting Eqs. (16), (18), and (21)–(24) together we can finally write down the total current contribution $I_2$ from the continuous spectrum

$$I_2=I_2^e+I_2^h=-\frac{2e}{h}\int_{\Delta_1}^{\sqrt{\mu^2+\Delta_1^2}}dE\frac{E}{\sqrt{E^2-\Delta_1^2}}\left(\left|a_5(E,\phi)\right|^2-\left|a_5(E,-\phi)\right|^2\right)\tanh\left(E/2k_BT\right). \tag{25}$$

To arrive at Eq. (25) we note that it is enough to integrate between $\Delta_1$ and $\sqrt{\mu^2+\Delta_1^2}$ in Eq. (16), simply because within the Andreev approximation $|a_5(E,\phi)|^2 = |a_5(E,-\phi)|^2 = 1$ for $E > \sqrt{\mu^2+\Delta_1^2}$.

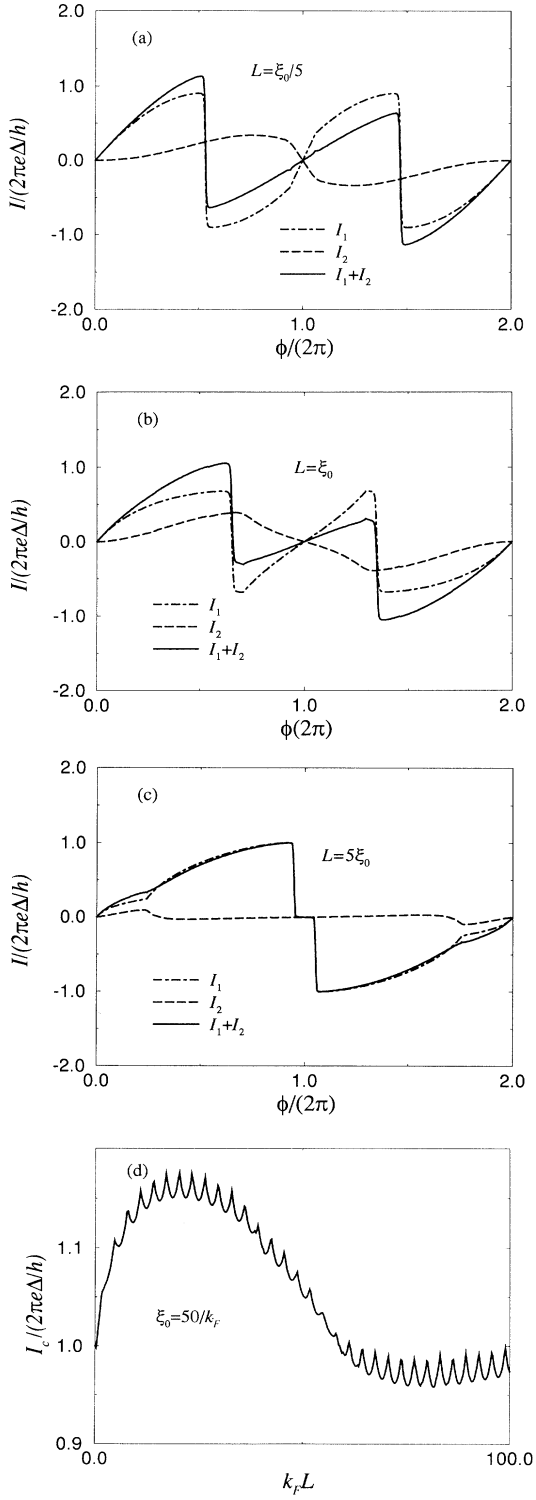


FIG. 5. In (a)–(c) the current contributions $I_1$ and $I_2$ as a function of $\phi$ for different $L$ are shown. In (d) the critical current $I_c$ as a function of $k_F L$ is shown.

## V. THE CURRENT

In this section we use Eqs. (3) and (25) to calculate the contributions from both the discrete and continuous spectrum, respectively. From now on we specialize to the case when the length $L_N$ of the N regions is zero, $L_N = 0$.

First we check the case $\Delta_1 = \Delta_3 = \Delta$, see Fig. 5. In Figs. 5(a)–5(c) we show how $I_1$ and $I_2$ compare to each other for different lengths. Also in Figs. 5(a)–5(c), the total current $I = I_1 + I_2$ is shown. For $L \ll \xi_0$, see Fig. 5(a), the contribution $I_2$ from the continuous spectrum is small (and zero for $L = 0$) compared to $I_1$. Increasing $L$, the ratio $I_2/I_1$ increases, reaching a peak at $\sim \xi_0$, see Fig. 5(b). For $L \gg \xi_0$ the ratio $I_2/I_1$ approaches zero and only $I_1$ contributes to the total current, see Fig. 5(c). In this case there is only one level per N region with the dispersion relation $E = \Delta \cos(\phi/4)$. From Eq. (3) we then have directly $I(\phi) = (e\Delta/\hbar)\sin(\phi/4)$ for $T = 0$, in agreement with the numerical calculations. In Fig. 5(d), the critical current $I_c$ as a function of length is shown. For small $L$, $I_c$ exceeds the value $e\Delta/\hbar$ for a short SNS junction, while for larger $L$ the limit $e\Delta/\hbar$ is approached. Therefore, introducing a third middle superconducting region with the same pair potential as in the superconducting electrodes does not change $I_c$ much, but rather redistributes the current contributions between the bound states ($I_1$) and the continuum ($I_2$). There are also oscillations in Fig. 5(d) on the scale of $k_F L \sim \pi$.

Next, we vary $\Delta_3$, keeping $L$ fixed. Putting $\Delta_3 = 0$ we can reproduce the known result for a long and clean SNS junction, where $I(\phi)$ is triangular in $\phi$. This case is discussed in detail in Ref. 5. In Fig. 6 the critical current $I_c$ as a function of $\Delta_3/\Delta_1$ is shown.

## VI. SUMMARY AND CONCLUDING REMARKS

In this paper we have studied the simplest case of stationary Josephson current through two coupled, ballistic SNS junctions by solving the one-dimensional BdG equation for a SNSNS structure. This allows us to go continuously between the two limits $L \gg \xi_0$ and $L \ll \xi_0$, where $L$ is the length of the middle S region.

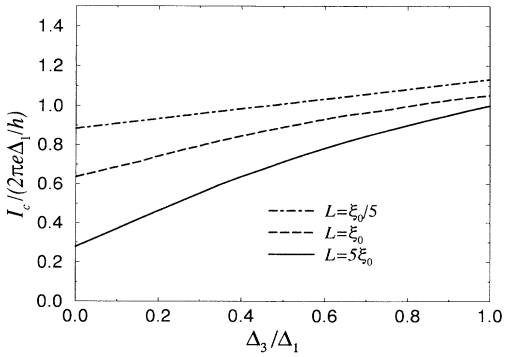


FIG. 6. The critical current $I_c$ as a function of $\Delta_3/\Delta_1$ for different $L$.

For $L \gg \xi_0$ our treatment describes two independent junctions with nonoverlapping Andreev states, only coupled via current conservation. As a result the critical current is unchanged compared to the single junction case ($I_c = e\Delta/\hbar$). There is one ($L_N = 0$) Andreev state for each junction. These two states are degenerate in this case. For $L \ll \xi_0$ (the strong coupling case) one approaches the single junction case with only a single bound Andreev state, which results in a $2\pi$ periodic dispersion relation for $L = 0$.

In the intermediate range $\xi_0 \sim L$, the bound Andreev states of each junction more or less overlap. The situation is analogous to bound states of a double quantum well, and the Andreev levels are split. We get "bonding" and "antibonding" combinations of bound Andreev states. The development from the weakly overlapping case to the strongly overlapping case is clearly demonstrated in Fig. 2. The upper level goes above the gap $\Delta$ when decreasing the distance $L$ between the junctions.

Our results show that, when $L \sim \xi_0$, it is essential to take into account the contribution $I_2$ from the continuous states, in addition to $I_1$. Only when $L \ll \xi_0$ or $L \gg \xi_0$ $I_2$ is negligible. The enhancement of the critical current, compared to $I_c = e\Delta/\hbar$ of the single junction, is technically due to the continuum current which adds to the current (and also subtracts at other phases $\phi$), see Fig. 5. In Fig. 7 we show the three cases discussed, plotted on the scale of the full $4\pi$ period.

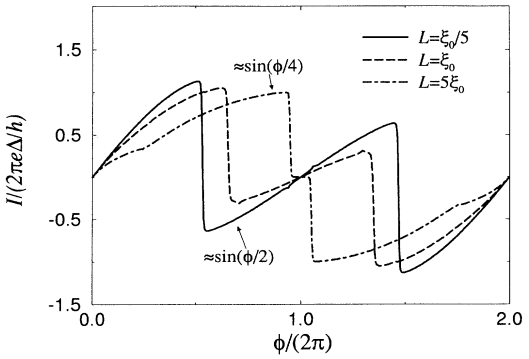


FIG. 7. Total current as a function of $\phi$ for three lengths $L$ of the middle S region ($\Delta_1 = \Delta_3 = \Delta$).

## ACKNOWLEDGMENTS

It is a pleasure to thank Vitaly Shumeiko for many discussions on various aspects of this work. This work has been supported by the Swedish Natural Science Research Council.

* Electronic address: hurd@fy.chalmers.se
† Electronic address: wendin@fy.chalmers.se

[1] B. D. Josephson, Phys. Lett. **1**, 251 (1962).
[2] P. W. Anderson and J. M. Rowell, Phys. Rev. Lett. **10**, 230 (1963).
[3] C. W. J. Beenakker, Phys. Rev. Lett. **67**, 3836 (1991).
[4] B. J. van Wees, K.-M. H. Lenssen, and C. J. P. M. Harmans, Phys. Rev. B **44**, 470 (1991).
[5] P. F. Bagwell, Phys. Rev. B **46**, 12573 (1992).
[6] R. Gross, in *Interfaces in Superconducting Systems*, edited by S. L. Shinde and D. Rudman (Springer-Verlag, New York, 1992).
[7] D. A. Wollman *et al.*, Phys. Rev. Lett. **71**, 2134 (1993).
[8] P. Chaudhari and S.-Y. Lin, Phys. Rev. Lett. **72**, 1084 (1994).
[9] I. O. Kulik, Zh. Eksp. Teor. Fiz. **57**, 1745 (1969) [Sov. Phys. JETP **30**, 944 (1970)].
[10] Y. Tanaka and M. Tsukada, Phys. Rev. B **44**, 7578 (1991).
[11] A. P. van Gelder, Phys. Rev. **181**, 787 (1969).
[12] H. Plehn, O.-J. Wacker, and R. Kümmel, Phys. Rev. B **49**, 12 140 (1994).
[13] E. Canel, Phys. Lett. **16**, 101 (1965).
[14] A. Martin-Rodero, F. J. Garcia-Vidal, and A. Levi Yeyati, Phys. Rev. Lett. **72**, 554 (1994).
[15] P. F. Bagwell, Phys. Rev. B **49**, 6841 (1994).
[16] F. Sols and J. Ferrer, Phys. Rev. **49**, 15 913 (1994).
[17] K. A. Matveev *et al.*, Phys. Rev. Lett. **70**, 2940 (1993).
[18] P. G. de Gennes, *Superconductivity of Metals and Alloys* (Addison-Wesley, New York, 1989).
[19] K. K. Likharev, Rev. Mod. Phys. **51**, 101 (1979).
[20] L.-F. Chang and P. F. Bagwell, Phys. Rev. B **49**, 15 853 (1994).
[21] M. Hurd and G. Wendin, Phys. Rev. B **49**, 15 258 (1994).
[22] G. E. Blonder, M. Tinkham, and T. M. Klapwijk, Phys. Rev. B **25**, 4515 (1982).
[23] M. Tinkham, Phys. Rev. B **6**, 1747 (1972).
[24] P. Johansson, Phys. Rev. B **46**, 12 865 (1992).